JET-INDUCED CIRCULATION AND DIFFUSION[a]

Discussion by Helmut Kobus

HELMUT KOBUS,[4] A. M. ASCE.—The authors are to be commended on their most valuable contribution to the problem of jet-induced circulation and on their lucid interpretation of the results in view of their application to bubble screens. The writer agrees that the analogy between the two types of flow is very close and hence much valuable information about the behavior of the latter can be obtained from the more simple study of the former. The differences, if any, are to be expected within the upward jet flow, while the pattern of induced circulatory motion should largely be the same in both cases under comparable conditions.

A recent experimental investigation by the writer of the upward flow induced by a bubble screen (7) has shown considerable deviations from the simplified model upon which the authors base their comparison between jet and bubble screens. To be sure, this does not necessarily mean that analogy does not exist; it just permits verification and specification of its conditions and limitations. The experiments comprise measurements of the vertical water velocities and of the mean rising speed u_b of the air bubble stream induced by a single and by rows of circular orifices. The orifices ranged in diameter from 0.5 mm to 5 mm and were operated at depths of 4.5 m below the free surface in a very large basin ($L/D \approx 20$; $B/D = 2$) at buoyancy inputs up to 4 kg per sec and 7 kg per sec m respectively. Because of the unstable config-

[a] March, 1969, by Constantin Iamandi and Hunter Rouse (Proc. Paper 6445).

[4] Oberingenieur, Institut für Hydromechanik, Universität Karlsruhe, Germany.

uration of bubble screen and eddies, velocities had to be time-averaged over a period of 5 min at each point. Water velocities were measured by an Ott current meter, and the mean rising speed of the air bubble stream was obtained from density measurements by means of radioisotopes.

Bubble screens are usually operated at depths of at least several meters below the free surface: the most frequent applications are connected with navigable waterways, where depths exceeding 10 m are not unusual. Furthermore, considerable rates of air flow are usually required to produce the desired effect. For this practical range of bubble screens, several striking

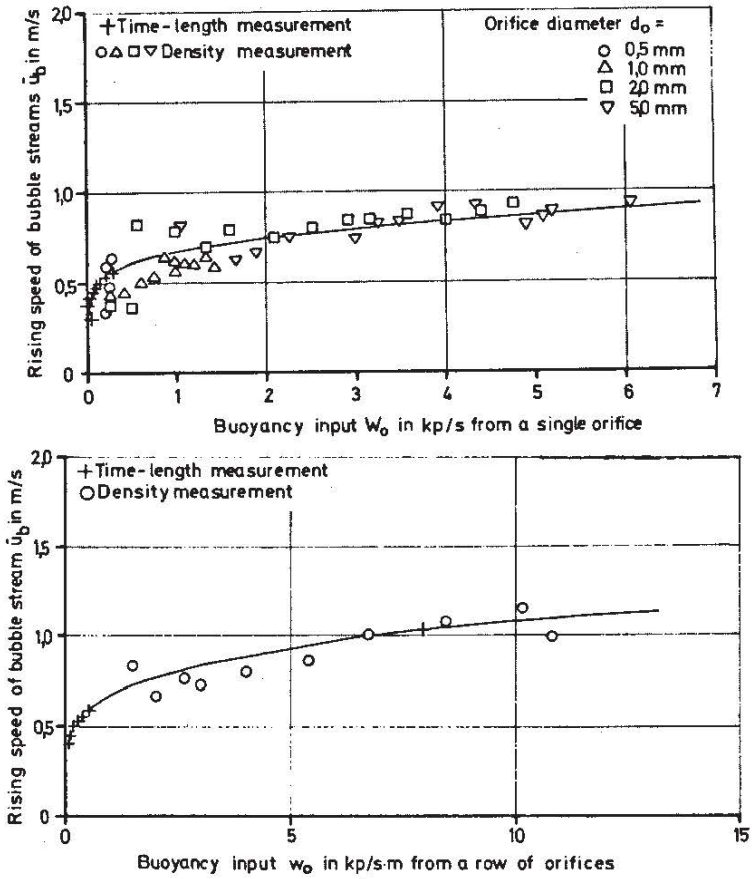

FIG. 9.—MEAN RISING SPEED $\bar{u}_b$ OF AIR-BUBBLE STREAM AS FUNCTION OF BUOYANCY INPUT

deviations from the simplified heat-convection model described in Ref. 6 can be noted:

1. Near the orifice, the continuous air stream discharging from the orifice breaks up into bubbles causing a very rapid initial expansion.
2. Bubbles of considerable size are generated, inducing relative motion between bubble and surrounding water. Hence, the assumption of infinitesimal bubble size does not apply.
3. The mean rising speed of the air bubbles—essential for the magnitude of the driving force—depends upon the air-discharge rate; as a consequence, the spread of water-velocity profiles also varies with the air-discharge rate.
4. The effects of compressibility are not negligible.

It has been shown (8) that the maximum bubble size generated by a contin-

uous air stream from an orifice depends solely upon the discharge rate and is independent of orifice size and fluid properties throughout the practical range of orifice diameters, i.e. from 0.5 to 5 mm. The maximum equivalent-sphere diameter is several centimeters; hence one might expect that the speed of rise of the bubble stream differs considerably from that of the surrounding liquid, and furthermore that the mean speed of rise of the bubble stream depends primarily upon the air-discharge rate and is independent of orifice size. Therefore, $\bar{u}_b$ was determined experimentally (Fig. 9). It is important to note that, in agreement with observations on single bubbles, the writer's measurements showed no significant change of the mean rising speed $\bar{u}_b$ of the air bubble stream with elevation outside an initial region near the orifice. For reasons of continuity, then, the mass flux of air should be the same at all consecutive cross sections. However, the buoyancy of some horizontal slice is given by the product of the total volume of air contained in the slice and the difference in specific weight of water and air, and although the change in air density will have practically no effect on the latter even at considerable water depths, the volume changes, directly proportional to the absolute pressure, may be considerable. If hydrostatic pressure distribution is assumed throughout the flow, the resulting ratio of buoyancy flux at some elevation x above the source to the buoyancy input is then given by,

$$\frac{w(x)}{w_0} = \frac{D^*}{D^* - x} \qquad (9)$$

in which $D^* = D + patm/\gamma w$ and the total momentum flux, neglecting the original contribution due to the source itself, by

$$m(x) = \int_0^x \frac{w(x)}{\bar{u}_b}\, dx = \frac{D^*\, w_0}{\bar{u}_b} \ln\left(\frac{D^*}{D^* - x}\right) \qquad (10)$$

This shows that, because of compressibility, the rate of momentum-flux increase with height is not linear although $\bar{u}_b$ has still been considered to be independent of elevation. One may thus conclude that the simple relationships derived in Ref. 6 do not apply here. The experiments verify this: while the measured velocity profiles are in accordance with the heatflow analogy insofar as they are described well by least-square-fit Gaussian distribution curves, a plot of the standard deviation σ against elevation (Fig. 10) shows that the spread of the profiles deviates considerably from the straight line according to Ref. 6 (The results for single orifices are shown also, because much more experimental information is available in that case). Near the origin, one can note a rapid expansion due to the breakup of the bubble stream. Beyond this initial region, the rate of spread is considerably smaller than predicted by the simplified analysis and is varying with the air-supply rate. The latter "concentration effect" causes a more rapid spread for higher air-supply rates. It is seen that the overall effect of the initial region can be represented by defining a "virtual origin," located a distance x_0 below the orifice. Beyond the initial region then, the spread of the velocity profiles increases linearly with distance from the virtual origin, the rate of spread c being a function of the air-supply rate.

Based upon experimental information about the distance x_0 between orifice and virtual origin, the rate of spread c of the velocity profiles, and the mean rising speed $\bar{u}_b$ of the bubble stream, a semiempirical approach has been used

(7) to obtain the water volume flux at any horizontal cross section. Since these three experimental quantities are independent of the distance from the origin, it is believed that extrapolation of the results to larger water depths should be permissible. Moreover, since the range of the experiments covers all practicable air-supply rates and orifice diameters, most practical air bubble installations should be within the scope of application of this approximate analysis.

By equating the expressions for the momentum flux obtained, respectively, from Eq. 10 and through integration of the velocity profiles, the resulting water volume flux at the surface due to a line source of air bubbles located at

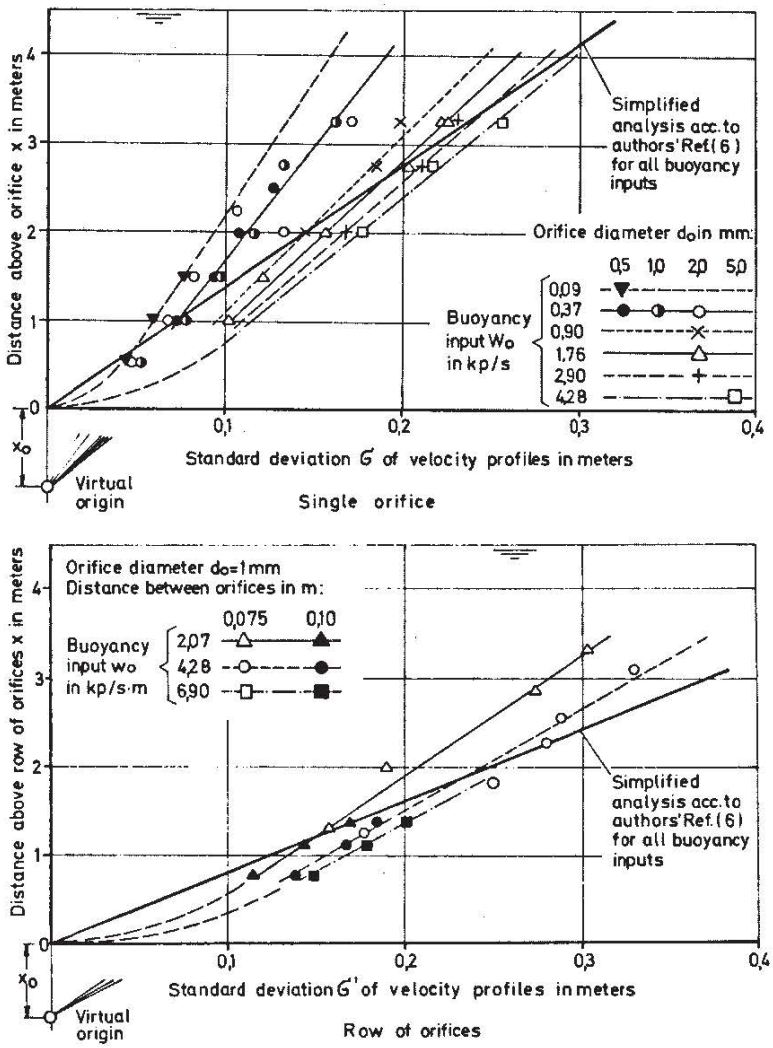

FIG. 10.—STANDARD DEVIATION OF GAUSSIAN VELOCITY PROFILES AS FUNCTION OF DISTANCE FROM ORIFICE AND BUOYANCY INPUT

a depth D below the free surface and producing an initial buoyancy w_0 per unit time and unit length is given by

$$q(D) = \left[\frac{2\sqrt{\pi}}{\rho w} D^*(D + x_0) \ln\left(\frac{D^* \gamma w}{patm}\right)\left(\frac{c}{\bar{u}_b}\right) w_0\right]^{1/2} \quad \ldots\ldots\ldots\ldots \quad (11)$$

From the experiments, it has been found that the value of x_0 is independent of w_0, and both c and $\bar{u}_b$ increase with about the 0.15 power of w_0. With the fraction $(c/\bar{u}_b)$ being approximately constant, then, $q(D)$ is seen to vary with the square root of the buoyancy input. The condition that the discharge rates at

the surface should be equal for the water jet and the bubble screen now leads to

$$\frac{m_0}{w_0}\sqrt{\frac{g}{D}}\,f(D) = 1 \quad \ldots\ldots\ldots\ldots\ldots\ldots\ldots\ldots\ldots\ldots\ldots\ldots \quad (12)$$

$$\text{with } f(D) = \frac{0.11\ D^2}{D^*(D + x_0)\ \ln\left(\frac{D^*\ \gamma w}{patm}\right)}\ \frac{\left(\frac{\bar{u}_b}{c}\right)}{\sqrt{gD}} \quad \ldots\ldots\ldots\ldots\ldots\ldots\ldots \quad (13)$$

in which $f(D)$ is proportional to $D^{-1/2}$ in first approximation. In Fig. 11, this expression is plotted and compared to the corresponding Eq. 5 by the authors for various water depths, D. It will be noted that the corresponding values for w_0 increase linearly with m_0 as compared to the authors' 1.5 power law, and that the preceding equation results in higher comparable air demands than the authors' equation. This is not surprising, since both the spread of the velocity profiles and the centerline-velocities as observed in the experiments were found to be smaller than the predicted values from the simplified analysis.

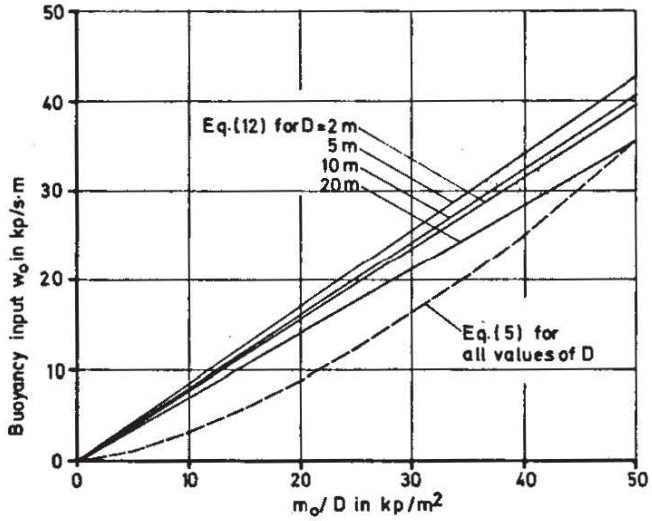

FIG. 11.—WATER-JET AND BUBBLE-SCREEN INPUTS GENERATING SAME RATE OF FLOW AT SURFACE

The authors' comparison of the efficiency of the two types of flow on the basis of the energy input required in either case warrants further comment. Rewriting Eq. 8 with the aid of Eq. 5, one obtains according to the simplified analysis

$$\frac{e_{0j}}{e_{0b}} = \frac{1}{2}\sqrt{\frac{D}{b_0}} \quad \ldots\ldots\ldots\ldots\ldots\ldots\ldots\ldots\ldots\ldots\ldots\ldots \quad (14)$$

As corresponding expression can be derived from Eq. 12 as

$$\frac{e_{0j}}{e_{0b}} = \frac{1}{2}\sqrt{\frac{D}{b_0}}\ \frac{\sqrt{\frac{m_0}{\gamma w}}}{D\ f(D)} \quad \ldots\ldots\ldots\ldots\ldots\ldots\ldots\ldots\ldots\ldots \quad (15)$$

Both equations indicate that the water jet requires considerably more energy input for small slot width ratios (b_0/D). For instance, a typical air-bubble installation would consist of 10 orifices per m of 1 mm diam,

corresponding to a slot width of 0.008 mm; at a water depth of 10 m, this would yield an energy-input ratio according to Eq. 14 of about 550. The more refined Eq. 15 yields smaller ratios due to the additional factor, which for most practical air-bubble installations would be of the order of 0.1 to 1. A further reduction results from the fact that the pressure drop across the nozzles, neglected in both expressions, can attain considerable magnitudes.

For a given rate of flow induction, an increase in slot width will decrease the required energy input for the water jet, while it affects the bubble-screen operation only insofar as the pressure drop at the nozzle diminishes. The authors' statement that the energy-flux ratio should be close to unity is therefore seen to be true only for large values of b_0/D, e.g. for 0.1 as suggested by the authors. It is important to note in this connection that, whereas the water jet requires an ever increasing discharge for larger slot widths and is hence limited by the capacity of the supply system, the bubble screen orifices can be increased in size without any increase in air demand, up to the point at which a continuous air discharge is barely possible.

The investigations described here support the authors' conclusions in general and suggest the following additional points:

1. In practical air-bubble installations, effects of finite bubble size and compressibility are not negligible and should be accounted for in the comparison of the two types of flow.
2. At small depths and input rates, water jet and air-bubble screen can be used alternatively with energy requirements of the same order of magnitude; for installations at large depths and input rates, it seems that bubble screens can be operated more efficiently.

Appendix.—References.

7. Kobus, Helmut, "Analysis of the Flow Induced by Bubble Screens," *Proceedings*, 11th Conference on Coastal Engrg., London, Sept., 1968.
8. Silberman, E., "Production of Bubbles by the Disintegration of Gas Jets in Liquids," *Proceedings*, 5th Midwestern Conference on Fluid Mechanics, Univ. of Michigan, 1957.

Errata.—The following correction should be made to the original paper:

Page 597, line 2: Should read $e_0 = \frac{\rho b_0 v_0^3}{2}$ instead of $e_0 = \rho b_0 v_0^{3/2}$